

# Ferroelectric $\text{PbTiO}_3/\text{SrRuO}_3$ superlattices with broken inversion symmetry

S.J. Callori,<sup>1</sup> J. Gabel,<sup>1</sup> Dong Su,<sup>2</sup> J. Sinsheimer,<sup>1</sup> M.V. Fernandez-Serra,<sup>1</sup> and M. Dawber<sup>1,\*</sup>

<sup>1</sup>*Department of Physics and Astronomy, Stony Brook University, Stony Brook, NY 11794-3800 USA*

<sup>2</sup>*Center for Functional Nanomaterials, Brookhaven National Laboratory, Upton, NY, USA*

We have fabricated  $\text{PbTiO}_3/\text{SrRuO}_3$  superlattices with ultra-thin  $\text{SrRuO}_3$  layers which act as dielectric, rather than metallic, elements. The superlattices display both ferroelectricity and, as the volume fraction of  $\text{PbTiO}_3$  is reduced, an increasingly important effect of polarization asymmetry due to compositional inversion symmetry breaking. The results are significant as they represent a new class of ferroelectric superlattices. By expanding our set of materials we are able to introduce new behaviors that can only occur when one of the materials is not a perovskite titanate. Here, compositional inversion symmetry breaking in bi-color superlattices, due to the combined variation of A and B site ions within the superlattice, is demonstrated using a combination of experimental measurements and first principles density functional theory.

Artificially layered perovskite oxide superlattices provide many opportunities to develop systems with novel and tunable properties[1, 2]. As far as ferroelectric superlattices are concerned, the insulating titanium perovskite oxides (e.g.  $\text{PbTiO}_3$ ,  $\text{BaTiO}_3$ ,  $\text{CaTiO}_3$  and  $\text{SrTiO}_3$ ) have to date been the most popular “building blocks”, but the need for new functionalities, particularly related to magnetism, requires the use of a wider set of materials and a deep understanding of the new physical phenomenon related to interfaces. In this letter an unconventional approach is demonstrated: we use a material that is normally metallic to play the role of a dielectric, in a ferroelectric-dielectric superlattice.

The much-studied compound  $\text{SrRuO}_3$  provides the proof of concept that metallic magnetic oxides can transform into thin-film dielectric components in certain heterostructures. In bulk,  $\text{SrRuO}_3$  has the distorted perovskite orthorhombic  $\text{Pnma}$  structure, is metallic and is ferromagnetic below  $T_c = 160$  K [3–7]. It is also a commonly used electrode material for oxides, and the interface with ferroelectric oxides has been much studied [8–12]. However,  $\text{SrRuO}_3$  becomes insulating in layers of thickness less than 4 unit cells; this behavior has been observed in thin films [13–15] and in  $\text{SrTiO}_3/\text{SrRuO}_3$  superlattices[16, 17]. First-principles investigations [18–20] and experiment [21–26] indicate that epitaxial strain, size effects, chemical pressure, surface reconstruction and interaction with the substrate may all play an important role in the observed behavior. We show in this letter that  $\text{PbTiO}_3/\text{SrRuO}_3$  superlattices containing single unit cell layers of  $\text{SrRuO}_3$  are insulating and can be ferroelectric.

A second motivation for creating  $\text{PbTiO}_3/\text{SrRuO}_3$  superlattices is that, as they have both A and B site variation, inversion symmetry can be compositionally broken [27, 28]. As a result, an asymmetry is introduced in the ferroelectric double well potential which can lead to “self-poling” materials. In a tri-color superlattice compositional breaking of inversion symmetry can occur with only A site variation, and has been demonstrated in superlattices containing  $\text{BaTiO}_3$ ,  $\text{CaTiO}_3$  and  $\text{SrTiO}_3$  [29, 30], but until now this behavior has not been shown

experimentally in bi-color superlattices.

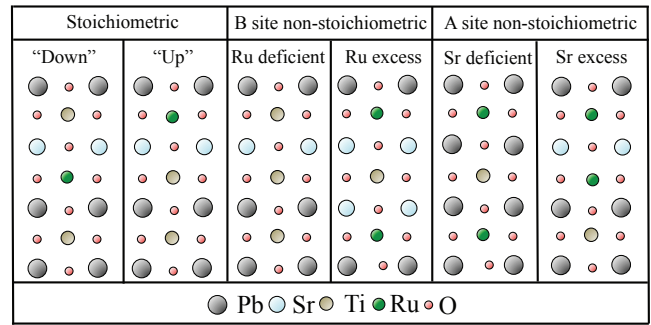


FIG. 1. Six possible interfaces that could form if off-stoichiometry can occur on either the A or B site within a  $\text{PbTiO}_3/\text{SrRuO}_3$  superlattice. The two labelled as “Stoichiometric” break inversion symmetry, and have a preference for either “Down” or “Up” polarization.

In  $\text{PbTiO}_3/\text{SrRuO}_3$  superlattices, stoichiometric interfaces will compositionally break inversion symmetry. However, as shown in Fig. 1., for the case of superlattices which contain a single unit cell layer of  $\text{SrRuO}_3$ , non-stoichiometry, which could occur on the local level, even in a sample which is globally stoichiometric, could lead to interfaces which maintain inversion symmetry. Any real sample will most likely contain several different kinds of interfaces, and our approach is therefore to identify, through a combination of experimental techniques and first principles calculations, which set of interfaces can best explain the observed characteristics of the superlattices.

Epitaxial growth of  $\text{PbTiO}_3/\text{SrRuO}_3$  superlattices can be achieved on  $\text{SrTiO}_3$  substrates as both  $\text{PbTiO}_3$  and  $\text{SrRuO}_3$  have in-plane lattice parameters close to that of  $\text{SrTiO}_3$ , which at room temperature is cubic with  $a=3.905$  Å. At room temperature bulk  $\text{PbTiO}_3$  is tetragonal ( $a=3.904$  Å,  $c=4.15$  Å) and orthorhombic  $\text{SrRuO}_3$  can be considered as pseudo-cubic with  $a=3.93$  Å. For this study, the  $n/1$   $\text{PbTiO}_3/\text{SrRuO}_3$  ( $n$  u.c.  $\text{PbTiO}_3/1$  u.c.  $\text{SrRuO}_3$ ) superlattices were deposited using off-axis

RF magnetron sputtering on (001) SrTiO<sub>3</sub> substrates, which had been treated with buffered HF to ensure TiO<sub>2</sub> termination. The SrRuO<sub>3</sub> layer thickness was grown to 1 u.c. for all the samples considered here, with the aim being that the SrRuO<sub>3</sub> layers should act as dielectrics, rather than metals. By contrast the thickness of the PbTiO<sub>3</sub> layer was changed from sample to sample, so that the relative effect of bulk ferroelectricity vs. interfacially driven compositional inversion symmetry breaking could be assessed. Our results are plotted in terms of the PbTiO<sub>3</sub> volume fraction, which is defined as the number of PbTiO<sub>3</sub> unit cells divided by the total number of unit cells in one PbTiO<sub>3</sub>/SrRuO<sub>3</sub> repetition. Growth rates for the two materials within the superlattice were obtained from x-ray diffraction measurements performed on many preliminary samples. Bottom SrRuO<sub>3</sub> electrodes (20 nm in thickness) were deposited *in situ* for the samples used for electrical measurements and gold top electrodes were added to the samples post-deposition. The superlattices were grown at a temperature of 550° C and the SrRuO<sub>3</sub> electrodes were grown at 620° C.

Experimentally, it has been demonstrated by Rjinders et al [31] that when grown by pulsed laser deposition the termination of a SrRuO<sub>3</sub> film is affected by both deposition conditions and layer thickness and that as a film grows on Ti terminated SrTiO<sub>3</sub> there is a conversion from a RuO<sub>2</sub> to a SrO termination layer. At a growth temperature of 700°C this transition already occurs for a single unit cell (u.c.) SrRuO<sub>3</sub> layer, but at lower deposition temperatures, this transition occurs later in the growth as the SrO layer is comparably more stable at these conditions. As a consequence of the small thickness of our SrRuO<sub>3</sub> layers, the low deposition temperatures used in our process, and the different kinetic regime of sputtering as compared to pulsed laser deposition, a RuO<sub>2</sub> termination of our SrRuO<sub>3</sub> layers, which is a pre-requisite for stoichiometric PbTiO<sub>3</sub>/SrRuO<sub>3</sub> superlattices, may still be possible.

The epitaxial growth of our samples was confirmed by x-ray diffraction and high resolution scanning transmission electron microscopy (HR STEM). Fig. 2 (a) shows a  $\theta/2\theta$  x-ray diffraction scan from a 6/1 PbTiO<sub>3</sub>/SrRuO<sub>3</sub> superlattice containing the 001 and 002 Bragg peaks, a simulation for a stoichiometric superlattice is also included in this figure for comparison. The x-ray diffraction data shown was performed using synchrotron radiation (10keV) at X22C at NSLS at BNL, and our routine characterizations of samples were performed on a Bruker D8 Discover diffractometer using Cu K- $\alpha$  radiation. The x-ray diffraction simulation shown was performed using kinematic theory, in a similar manner to Thompson et al [32]. In general we found that in terms of agreement between simulated and experimental peak intensities simulations for superlattices with non-stoichiometric interfaces were poorer matches to the experiment than simulation for stoichiometric superlattices.

Fig. 2(b) shows a HR STEM cross section of a 9/1 PbTiO<sub>3</sub>/SrRuO<sub>3</sub> superlattice. As can be seen the brightness of the layers, which is proportional to the atomic number of the atoms in the layers, is quite different to that of the substrate. The PbTiO<sub>3</sub> layers are the brightest because of the high atomic number of Pb, while the SrRuO<sub>3</sub> layers are less bright than PbTiO<sub>3</sub>, but have enhanced brightness compared to SrTiO<sub>3</sub> (not shown) because the Ru ion has a higher atomic number than Ti. The STEM image demonstrates that all 4 of the main cations are present in close to stoichiometric proportions.

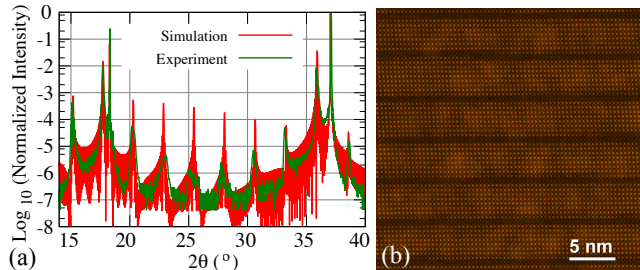


FIG. 2. (a) A  $2\theta/\theta$  x-ray diffraction scan on a 6/1 PbTiO<sub>3</sub>/SrRuO<sub>3</sub> superlattice showing the 001 and 002 Bragg peaks, as well as superlattice satellite peaks. (b) A HR-STEM image of a 9/1 PbTiO<sub>3</sub>/SrRuO<sub>3</sub> superlattice.

Support for the conclusion that our superlattices break compositional inversion symmetry comes from first principles calculations. These were performed using density functional theory, using a basis of numerical atomic orbitals as implemented in the SIESTA code. We used the same the same basis set and pseudopotentials as Junquera et al[34]. The results shown here were obtained within the local density approximation (LDA), although we have also studied the influence of spin polarization, the use of the generalized gradients approximation within the commonly used Wu-Cohen parametrization[35], and the effect of correlations within the LDA+U approximation[36], none of which have a significant impact on the conclusions of this paper. Full details regarding the calculations can be found in the supplemental materials to this letter[37].

From our first principles calculations we have determined the formation energy for superlattices with Sr excess and Ru excess interfaces and compared it to that of stoichiometric interfaces. The formation energy is defined as,  $E_{formation}(SL) = E_{total}(SL) - \sum_{uc=1}^n E_{total}(uc)$ , where  $E_{total}(SL)$  describes the total energy of the entire superlattice and  $E_{total}(uc)$  is the total energy of each of the  $n$  perovskite unit cells that compose the superlattice. The total energy of a single unit cell is computed in a bulk relaxation calculation of this unit cell restricted to the same symmetry and strain conditions as the superlattice. In Table 1 we show the relative formation

energy,  $\Delta E_{formation}$ , for Sr and Ru excess interfaces, which is found by subtracting the value for the interface being considered from the value for the stoichiometric interface[37]. A positive  $\Delta E_{formation}$  indicates that the stoichiometric (symmetry breaking) interface is more stable. For most superlattices, especially for those with high  $\text{PbTiO}_3$  volume fractions the stoichiometric interface is energetically preferred.

Superlattice	$\Delta E_{formation}$ (eV)	
	Ru excess	Sr excess
$(\text{PbTiO}_3)_2(\text{SrRuO}_3)_1$	+0.057	-0.020
$(\text{PbTiO}_3)_3(\text{SrRuO}_3)_1$	+0.040	-0.014
$(\text{PbTiO}_3)_5(\text{SrRuO}_3)_1$	+0.077	+0.009
$(\text{PbTiO}_3)_6(\text{SrRuO}_3)_1$	+0.081	+0.035
$(\text{PbTiO}_3)_7(\text{SrRuO}_3)_1$	-	+0.063
$(\text{PbTiO}_3)_9(\text{SrRuO}_3)_1$	-	+0.096

TABLE I. Theoretical formation energies for the symmetry preserving (Ru and Sr excess) structures compared to the symmetry breaking stoichiometric superlattices. The DFT calculations were performed within the LDA approximation.

In the two-component  $\text{PbTiO}_3/\text{SrRuO}_3$  superlattices in which the inversion symmetry is broken by the stoichiometric interface structure our calculations predict a self-poling behavior. In Fig. 3 we show the energy of the superlattice as a function of the polarization. This was produced by calculating the total energy of the system for atomic displacements along the line  $\vec{r} = \vec{r}_{P_+} + u(\vec{r}_{P_-} - \vec{r}_{P_+})$  interpolating linearly between the two minima of the energy. These two minima are characterized by two different polarization states,  $P_{up}$  (higher energy minimum) and  $P_{down}$  (lower energy minimum). As shown in Table II, the simulations for the stoichiometric interface show that, as the volume fraction is reduced, there is an increasingly large difference in the values of the stable up and down polarizations, until for the 5/1 superlattice only the down polarization is stable.

Superlattice	Stable Polarization ( $\mu\text{C}/\text{cm}^2$ )	
	$P_{down}$	$P_{up}$
$(\text{PbTiO}_3)_5(\text{SrRuO}_3)_1$	35.8	unstable
$(\text{PbTiO}_3)_6(\text{SrRuO}_3)_1$	39.2	16.8
$(\text{PbTiO}_3)_7(\text{SrRuO}_3)_1$	45.0	45.1
$(\text{PbTiO}_3)_9(\text{SrRuO}_3)_1$	50.9	50.2

TABLE II. Calculated stable polarization magnitudes (DFT LDA) in the up and down directions for a selection of stoichiometric superlattices.

Experimental values for the ferroelectric polarization of the samples were obtained from polarization-electric field hysteresis loops performed on a number of samples. Polarization hysteresis was observed in samples with a  $\text{PbTiO}_3$  layer thickness of 5 u.c or greater, (ie. for vol-

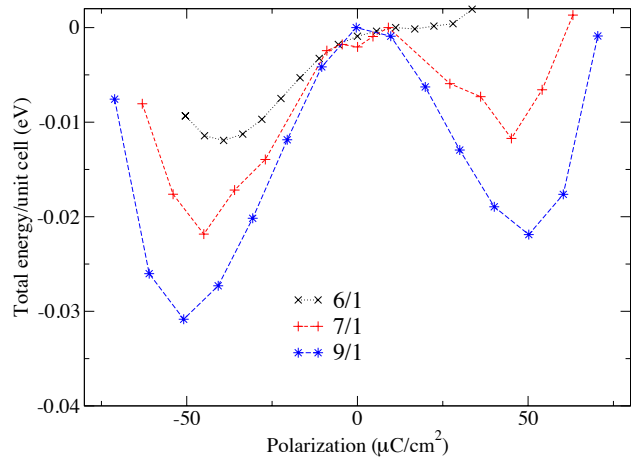


FIG. 3. Calculated total energy per unit cell as a function of polarization.

ume fractions greater than 82%). Characteristic loops measured at 3 different frequencies on the 7/1 sample are shown as an inset to Fig. 4. Successful hysteresis loops confirm that the thin layers of  $\text{SrRuO}_3$  in the material are acting as dielectric layers, and allow a continuous polarization in the structure. An independent confirmation of ferroelectricity comes from x-ray diffraction reciprocal space maps around superlattice Bragg peaks, shown in the supplemental information[37]. These show diffuse scattering from the in-plane periodicity of stripe domains with polarization oriented up and down with respect to the substrate, and are similar to those seen in  $\text{PbTiO}_3/\text{SrTiO}_3$  superlattices.[38, 39]. These domain features were observed in the 7/1, 9/1, and 13/1 superlattices, but not in the 5/1 superlattice. The lack of domain features in the 5/1  $\text{PbTiO}_3/\text{SrRuO}_3$  superlattice may be due to the relative instability of one polarization state with respect to each other, ie., while the polarization can be switched under field from one direction to the other, its equilibrium configuration is dominated by a single polarization direction.

The experimentally measured polarization as a function of the  $\text{PbTiO}_3$  volume fraction is plotted in Fig. 4 along with results for three different kinds of interface from DFT LDA simulations. The polarization values labelled as theory in Fig. 4 correspond to half of the sum of the magnitudes of the calculated polarization in the up and down direction, which should correspond to the switched polarization, which is what is measured in a polarization-field hysteresis loop. The DFT calculations are at zero temperature, while the experimental measurements are performed at room temperature, and so it is expected that the calculated values of polarization exceed the measured ones for all volume fractions, and that ferroelectricity should persist to lower volume fractions for theoretical superlattices than in experiment. This is the

case for the calculations of both stoichiometric and Ru excess superlattices, but the values calculated for the Sr excess superlattices drop off much more rapidly than the experimental values as the volume fraction is reduced.

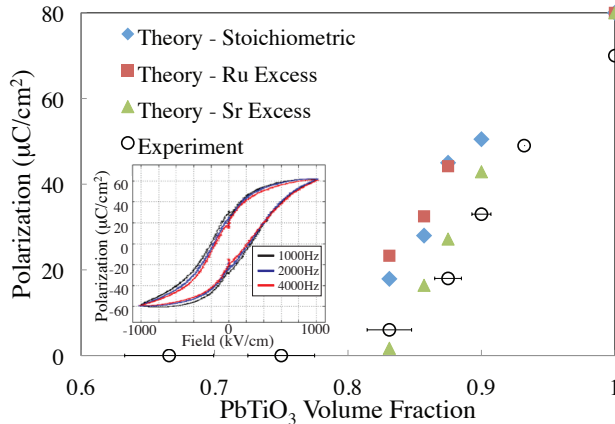


FIG. 4. Switched polarization plotted as a function of the  $\text{PbTiO}_3$  volume fraction. Inset: Polarization-field hysteresis loops measured at 3 different frequencies on a 7/1 sample.

The average tetragonality ( $c/a$ ) of ferroelectric superlattices is related to the polarization and can be used as an additional probe of ferroelectric properties [40–42]. This was measured by x-ray diffraction and compared to the first principles results. The plot of  $c/a$  versus  $\text{PbTiO}_3$  volume fraction shows two regimes. For volume fractions less than approximately 80%  $\text{PbTiO}_3$  the  $c/a$  of the superlattices is less than that of a 20 nm  $\text{SrRuO}_3$  thin film. At these volume fractions, the  $\text{PbTiO}_3$  layers are paraelectric, and therefore do not display the enhanced tetragonality of ferroelectric  $\text{PbTiO}_3$ . Above this volume fraction, the samples are ferroelectric and display the corresponding  $c/a$  increase. Fig. 5 shows the experimental  $c/a$  values, as well as simulated data for  $\text{PbTiO}_3/\text{SrRuO}_3$  superlattices with the three different kinds of interfaces. When the comparison between theory and experiment is made over the whole range of the plot the trend of the experimental results seems to match the prediction for the stoichiometric case significantly better than either non-stoichiometric case.

The effect that the compositional breaking of inversion symmetry has on functional properties is most evident in the dielectric response of the samples. In Fig. 6, we show dielectric constant measured as a function of electric field (at a frequency of 10kHz). The measurements show an evolution from a typical butterfly loop for  $\text{PbTiO}_3$  rich samples (13/1 and 9/1 samples) to a highly asymmetric curve with greatly enhanced peak dielectric constant for the 3/1 sample. An unusual characteristic where two peaks are seen on each voltage trace displayed in the 5/1 sample. The composition at which the transition from conventional ferroelectric behavior occurs (approx. 7/1) matches the composition highlighted by the-

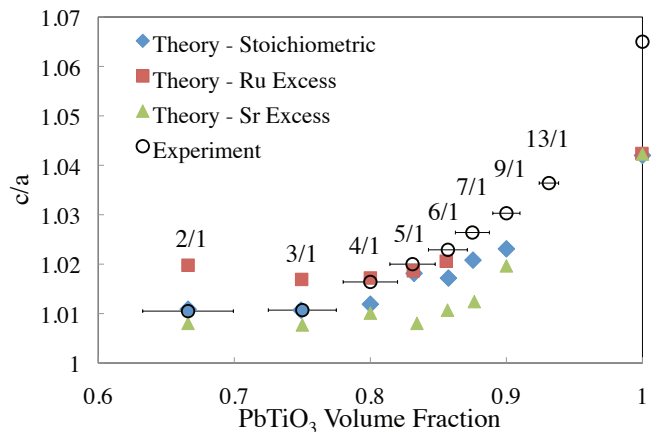


FIG. 5. Average tetragonality, or the ratio of the average out of plane lattice parameter  $c$  to the lattice parameter of the  $\text{SrTiO}_3$  substrate  $a$  ( $c/a$ ) plotted as a function of  $\text{PbTiO}_3$  volume fraction. As well as the experimental results results from DFT LDA calculations for three different kinds of interfaces are shown.

ory at which compositional inversion symmetry breaking becomes a dominant factor. To summarize our picture of this system: The 3/1 sample can be characterized as a spontaneously polarized non-switchable insulator (or, in other words, an interfacially driven pyroelectric). Samples between 7/1 and 3/1 are best described as asymmetric ferroelectrics. Samples with volume fractions above 7/1, while still containing interfaces which compositionally break inversion symmetry are not greatly affected by them.

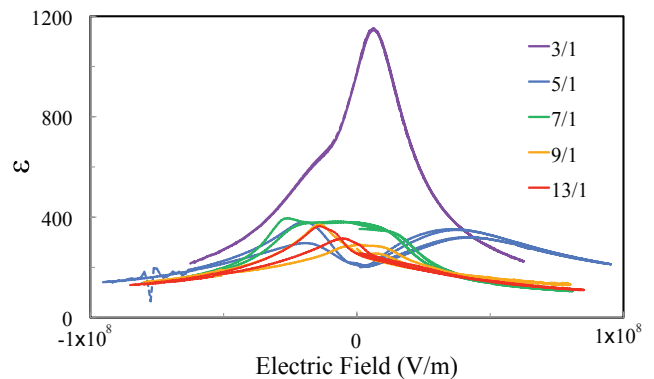


FIG. 6. Dielectric constant-field loops for 5 of our samples.

Our results demonstrate the possibilities unlocked by expanding our material set for ferroelectric superlattices. Here it has been shown that materials such as  $\text{SrRuO}_3$  can have significantly different properties to their bulk forms when incorporated in to ferroelectric superlattices. This finding should motivate a broader exploration of candidate materials for the development of new artificially layered ferroelectrics. In particular, the use of thin

metallic materials as dielectrics has intriguing potential for the development of highly coupled multiferroics. The importance of stoichiometry at interfaces has also been considered. We have shown that that when this can be maintained compositional inversion symmetry breaking can be achieved in a bi-color superlattice.

MD acknowledges support from the National Science Foundation under DMR1055413. MD and DS acknowledge support from a SBU/BNL seed grant. MVFS acknowledges support from DOE award DEFG02-09ER16052. Use of the National Synchrotron Light Source and the Center for Functional Nanomaterials, at Brookhaven National Laboratory, was supported by U.S. Department of Energy, Office of Basic Energy Sciences, under Contract No. DE-AC02-98CH10886.

---

\* matthew.dawber@stonybrook.edu

- [1] M. Dawber, N. Stucki, C. Lichtensteiger, S. Gariglio and J.-M. Triscone, *J. Phys. Condens. Matter* **20** 264015 (2008).
- [2] P. Zubko, S. Gariglio, M. Gabay, P. Ghosez and J.-M. Triscone, *Annu. Rev. Condens. Matter. Phys.*, **2** 141 (2011).
- [3] P.B. Allen, H. Berger, O. Chauvet, L. Forro, T. Jarlborg, A. Junod, B. Revaz and G. Santi, *Phys. Rev. B*, **53** 4393 (1996).
- [4] D. J. Singh, *J. Appl. Phys.* **79**, 4818 (1996).
- [5] I. I. Mazin and D.J. Singh, *Phys. Rev. B* **56**, 2556 (1997).
- [6] J.S. Dodge, C.P. Weber, J. Corson, J. Orenstein, Z. Schlesinger, J.W. Reiner and M.R. Beasley, *Phys. Rev. Lett.* **85**, 4932 (2000).
- [7] L. Capogna, A. P. Mackenzie, R.S. Perry, S.A. Grigera, L.M. Galvin, P. Raychaudhuri, A.J. Schofield, C.S. Alexander, G. Cao, S.R. Julian and Y. Maeno, *Phys. Rev. Lett.* **88**, 076602 (2002).
- [8] J. Junquera and P. Ghosez, *Nature* **422**, 506 (2003).
- [9] G. Gerra, A. K. Tagantsev, N. Setter, and K. Parlinski, *Phys. Rev. Lett.* **96** 107603 (2006).
- [10] M. Stengel and N. A. Spaldin, *Nature* **443**, 679 (2006).
- [11] P. Aguado-Puente, J. Junquera, *Phys. Rev. Lett.* **100** 177601 (2008).
- [12] J. Shin, A. Borisevich, V. Meunier, J. Zhou, E. W. Plummer, S.V. Kalinin and A.P. Baddorf, *ACS Nano* **4**, 4190 (2010).
- [13] D. Toyota, I. Ohkubo, H. Kumigashira, M. Oshima, T. Ohnishi, M. Lippmaa, M. Kawasaki, and H. Koinuma, *Appl. Phys. Lett.* **87**, 162508 (2005), *J. Appl. Phys* **99** 08N505 (2006).
- [14] M. Schultz, S. Levy, J.W. Reiner and L. Klein, *Phys. Rev. B* **79** 125444 (2009).
- [15] J. Xia, W. Siemons, G. Koster, M.R. Beasley and A. Kapitulnik, *Phys. Rev. B* **79**, 140407(R) (2009).
- [16] M. Izumi, K. Nakazawa and Y. Bando, *J. Phys. Soc. Japan* **67** 651 (1998).
- [17] H. Kumigashira, M. Minohara, M. Takizawa, A. Fujimori, D. Toyota, I. Ohkubo, M. Oshima, M. Lippmaa, and M. Kawasaki, *Appl. Phys. Lett.* **92** 122105 (2008).
- [18] A. T. Zayak, X. Huang, J. B. Neaton, and Karin M. Rabe, *Phys. Rev. B* **74** 094104 (2006), *Phys. Rev. B* **77**, 214410 (2008) .
- [19] J. M. Rondinelli, N. M. Caffrey, S. Sanvito and N. A. Spaldin, *Phys. Rev. B* **78** 155107 (2008).
- [20] P. Mahadevan, F. Aryasetiawan, A. Janotti, T. Sasaki , *Phys. Rev. B* **80**, 035106 (2009).
- [21] G. Herranz, B. Martinez, J. Fontcuberta, F. Sanchez, C. Ferrater, M.V. Garcia-Cuenca, M Varela *Phys. Rev. B* **67** 174423 (2003).
- [22] K.W. Kim, J.S. Lee, T. W. Noh, S.R. Lee and K. Char, *Phys. Rev. B* **71** 125104 (2005).
- [23] R. G. Moore, Jiandi Zhang, V. B. Nascimento, R. Jin, Jiandong Guo, G.T. Wang, Z. Fang, D. Mandrus, E. W. Plummer, *Science* **26** 318, 615 (2007).
- [24] A. Grutter, F. Wong, E. Arenholz, M. Liberati, and Y. Sukuki, *J. Appl. Phys.* **107** 09E138 (2010).
- [25] M. Ziese, I. Vrejoiu and D. Hesse, *Phys. Rev. B* **81** 184418 (2010).
- [26] K. J. Choi, S. H. Baek, H. W. Jang, L. J. Belenky, M. Lyubchenko, and C.-B. Eom, *Adv. Mater.* **22** 759762 (2010).
- [27] N. Sai, B. Meyer, and D. Vanderbilt, *Phys. Rev. Lett.*, **84**, 5636 (2000).
- [28] N. Sai, B. Meyer, and D. Vanderbilt, *Fundamental Physics of Ferroelectrics*, , 218 (2001).
- [29] M.P. Warusawithana, E.V. Colla, J.N. Eckstein, and M. B. Weissman *Phys. Rev. Lett.* **90** 036802 (2003).
- [30] H.N. Lee, H.M. Christen, M.F. Chisholm, C.M. Rouleau and D.H. Lowndes, *Nature* **433**, 395 (2005).
- [31] G. Rijnders, D.H.A. Blank, J. Choi, and C.B. Eom, *Appl. Phys. Lett.*, **84**, 505 (2004).
- [32] C. Thompson, C.M. Foster, J.A. Eastman and G.B. Stephenson. *Appl. Phys. Lett.*, **71** 3156 (1997).
- [33] J.M. Soler, E. Artacho, J.D. Gale, A. García, J. Junquera, P. Ordejón, and D. Sánchez-Portal, *J. Phys. Condens. Matter* **14** 2745 (2002).
- [34] J. Junquera, M. Zimmer, P. Ordejón, Ph. Ghosez, *Phys. Rev. B* **67** 155327 (2003).
- [35] Z. Wu and R.E. Cohen, *Phys. Rev. B*. **73** 235116 (2006).
- [36] M. Wierzbowska, D. Sanchez-Portal, and S. Sanvito. *Phys. Rev. B* **70** 235209 (2004).
- [37] Details in Supplementary Materials.
- [38] P. Zubko, N. Stucki, C. Lichtensteiger, and J.-M. Triscone, *Phys. Rev. Lett.*, **104**, 187601 (2010).
- [39] J.Y. Jo, P.Chen, R.J. Sichel, S.J. Callori, J. Sinsheimer, E.M. Dufresne, M. Dawber and P.G. Evans, *Phys. Rev. Lett.*, **107** 055501 (2011).
- [40] M. Dawber, C. Lichtensteiger, M. Cantoni, M. Veithen, P. Ghosez, K. Johnston, K.M. Rabe, and J.-M. Triscone, *Phys. Rev. Lett.*, **95**, 177601 (2005).
- [41] M. Dawber, N. Stucki, C. Lichtensteiger, S. Gariglio, P. Ghosez and J.-M. Triscone, *Advanced Materials*, **19**, 4153 (2007).
- [42] E. Bousquet, M. Dawber, N. Stucki, C. Lichtensteiger, P. Hermet, S.Gariglio, J.-M. Triscone, and P. Ghosez, *Nature*, **452**, 732 (2008).